Supporting Information

for

Quenching of Spin Polarization Switching in Organic Multiferroic Tunnel Junctions by Ferroelectric "Ailing-Channel" in Organic Barrier

Shiheng Liang[1,2], Zhongwei Yu[1,7], Xavier Devaux[1], Anthony Ferri[3], Weichuan Huang[4], Huaiwen Yang[1], Rachel Desfeux[3], Xiaoguang Li[4], Sylvie Migot[1], Debapriya Chaudhuri[5], Hongxin Yang[6], Mairbek Chshiev[5], Changping Yang[2], Bin Zhou[2], Jinghuai Fang[7], Stéphane Mangin[1] and Yuan Lu[1*]

[1]*Institut Jean Lamour, UMR 7198, CNRS-Université de Lorraine, Campus ARTEM, 2 Allée André Guinier, BP 50840, 54011 Nancy, France*

[2]*Department of Physics, Hubei University, Wuhan 430062, P. R. China*

[3]*Univ. Artois, CNRS, Centrale Lille, ENSCL, Univ. Lille, UMR 8181, Unité de Catalyse et Chimie du Solide (UCCS), F-62300 Lens, France*

[4]*Hefei National Laboratory for Physical Sciences at the Microscale, Department of Physics, University of Science and Technology of China, Hefei 230026, P. R. China*

[5]*Univ. Grenoble Alpes, INAC-SPINTEC, F-38000 Grenoble, France; CEA, INAC-SPINTEC, F-38000 Grenoble, France; CNRS, SPINTEC F-38000 Grenoble, France*

[6]*Key Laboratory of Magnetic Materials and Devices, Ningbo Institute of Materials Technology and Engineering, Chinese Academy of Sciences, Ningbo, 315201, China*

[7]*School of Science, Nantong University, 9 Seyuan Road, Nantong 226019, P. R. China*

** Corresponding author: yuan.lu@univ-lorraine.fr*

S1. Top electrode deposition with Liq-N_2 cooling technique

The top Au/Co electrodes were deposited in the MBE system (with a base pressure of 1×10^{-10} torr) by e-beam evaporation. On the purpose of further improvement of P(VDF-TrFE) quality, the sample was annealed at 120°C for one hour under high vacuum before decreasing temperature for Au/Co deposition. To minimize the metal diffusion into organic barrier, the deposition temperature of Au/Co is maintained at around 80K by cooling the sample with injection of Liq-N_2 through the sample holder, as shown **Figure S1**.

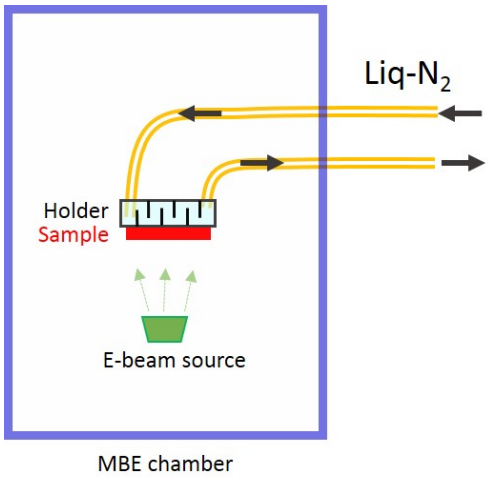

Figure S1. Schematic of MBE deposition with keeping sample's temperature at ~80K, with injection of Liq-N2 into the holder which tightly contacts with sample.

S2. STEM and EELS mapping on the *medium* P(VDF-TrFE) samples.

Figure S2a presents STEM image of the OMFTJ stack structure with *medium* thickness of P(VDF-TrFE). Compared to the *thin* sample, the thickness of the organic barrier appears much homogenous in the *medium* sample. No obvious "pot-hole" structure is found in the observed region. This also validates the ferroelectric switching homogeneity measured by PFM phase mapping (see **Figure 4d** in main text).

EELS spectra were also recorded to study the distribution of the elements. **Figure S2b** shows an ADF STEM image where EELS spectrum image was recorded. For the three regions marked with 1, 2 and 3 on the STEM image, EELS spectra are collected and presented in **Figure S2c**. Although the Co signal is well distinguished in the region close to Co/P(VDF-TrFE) interface (No.1), we cannot find any Co signal in the middle of P(VDF-TrFE) barrier (No.2). There are also no La and Mn signals in P(VDF-TrFE) barrier compared to the strong signals from the region close to P(VDF-TrFE)/LSMO interface (No.3). All these results prove that there is no metal diffusion into the P(VDF-TrFE) organic barrier when Au/Co electrode is deposited at low temperature.

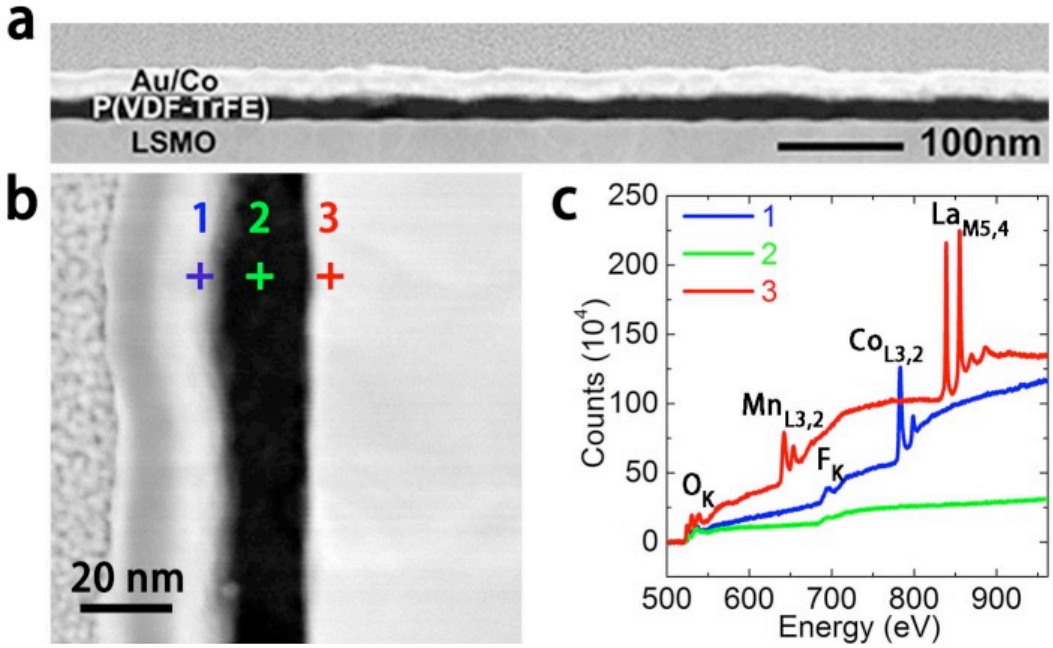

Figure S2. Large scale (a) and magnified (b) ADF STEM images of LSMO/P(VDF-TrFE)(*t* =19nm)/Co device. (c) EELS spectra recorded on the areas indicated in the STEM image (b).

S3. EDS characterization on the thin P(VDF-TrFE) sample.

Here, we show more STEM images of the *thin* sample and we performed another chemical analysis technique: energy dispersive spectroscopy (EDS) to double check the Co diffusion in the organic barrier. **Figure S3** and **S4** display the STEM images in different regions and the EDS analysis in different zones. Our conclusion is again that the Co diffusion is very limited in the P(VDF-TrFE) barrier. The suppression of Co diffusion in the P(VDF-TrFE) barrier is due to the low temperature growth (80K) of Au/Co electrode.

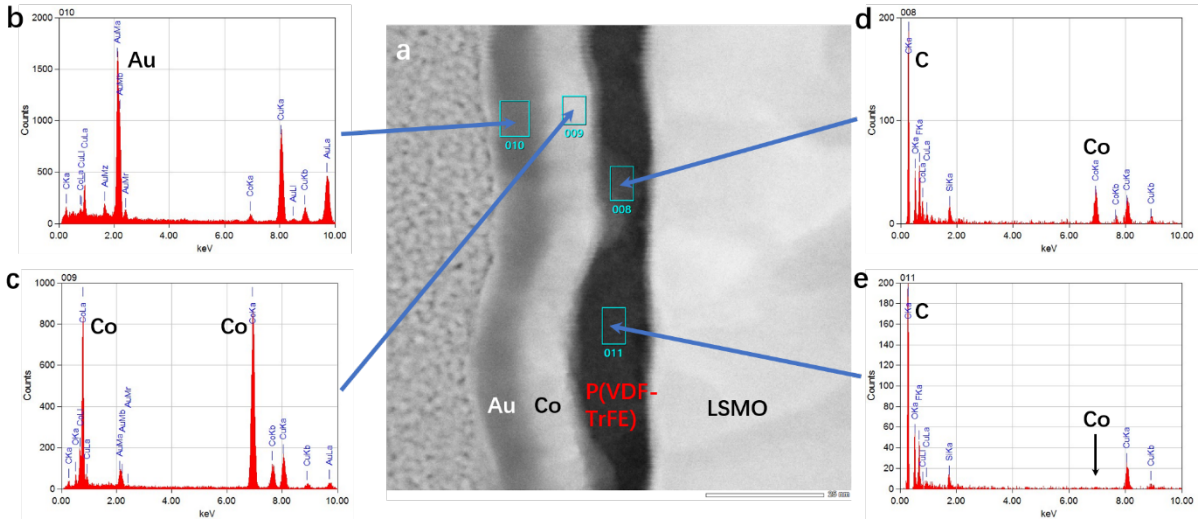

Figure S3. (a) ADF STEM image of the *thin* sample and EDS analysis on different zones in (b) Au layer, (c) Co layer, (d) Co and P(VDF-TrFE) superposition zone, and (e) P(VDF-TrFE) barrier.

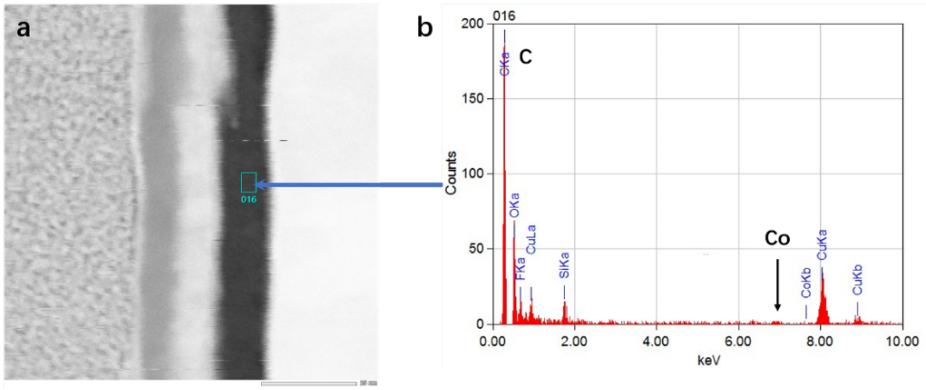

Figure S4. (a) ADF STEM image of the *thin* sample and (b) EDS analysis in the P(VDF-TrFE) barrier.

S4. Verification of pinhole contribution

A. Conductive AFM mapping of barrier conductivity.

Conductive AFM measurement is the most direct way to identify the existence of pinholes. Nanoscale conductivity variations were probed through current mapping experiments using the conductive-AFM (c-AFM) technique. A Ti/Ir-coated silicon tip and cantilever with a stiffness of $3 N \cdot m^{-1}$ were used. DC bias voltages ranging from -10 and +10V between the grounded AFM tip and the bottom electrode were applied during scanning. The electrical conductivity was locally probed over the surface of the P(VDF-TrFE) layer by using c-AFM mode. The current map recorded over 20x20 µm² large area are displayed in **Figure S5** for the samples with different P(VDF-TrFE) thicknesses. No conducting path is obtained for an applied bias of +5V, as demonstrated by the uniform contrast associated to insignificant current. Such absence of conduction signal was confirmed in several places of the sample surface regardless the applied bias voltage when varying between -10 and +10V, which confirms that the contribution of pinhole on transport is very limited. This also proves that the polarizing voltage around ±2V range does not induce a damage of organic barrier with the formation of pinholes and leakage currents.

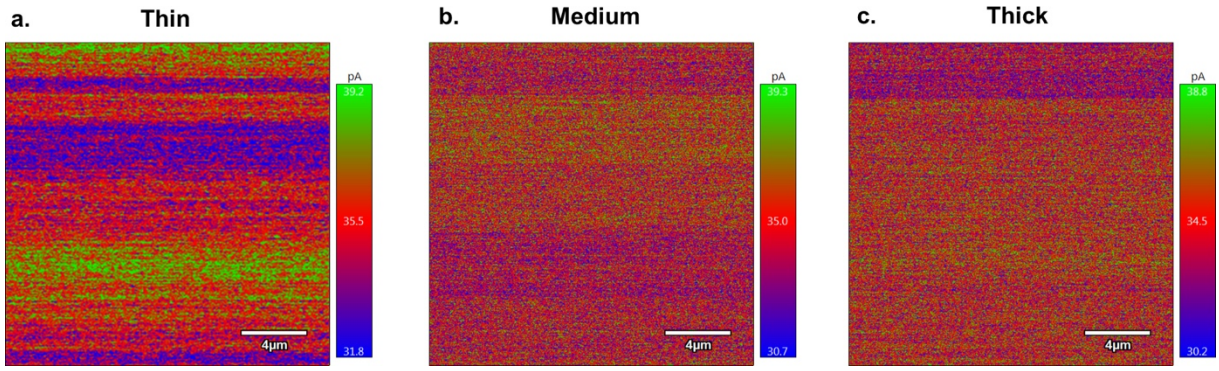

Figure S5. C-AFM scanning of barrier conductivity under an applied bias of +5V for different thickness of P(VDF-TrFE)(t) samples: (a) t = 15nm, (b) t = 19nm and (c) t = 33nm.

B. Non-linear IV curve.

Figure S6 shows the *I-V* characteristic of the devices with different thicknesses measured in negative polarized state. It can be seen that all *I-V* curves of the three samples show non-linear properties which indicates a tunneling behavior.

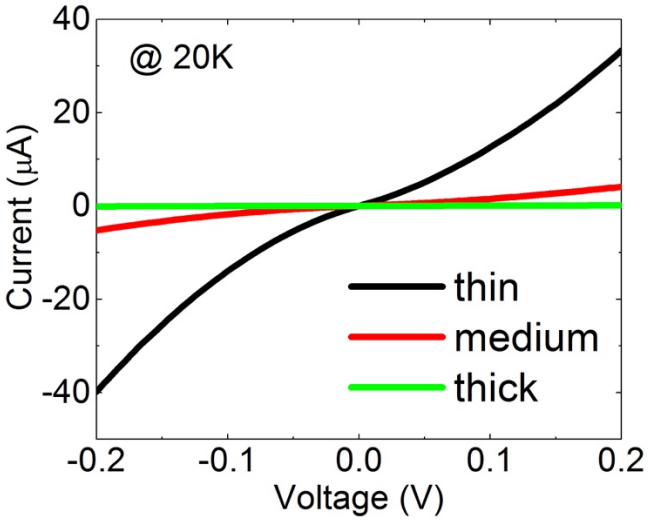

Figure S6. *I-V* characteristics under the range between -0.2V to 0.2V for devices of LSMO/P(VDF-TrFE)(*t*)/Co, (a) *t* = 15nm, (b) *t* = 19nm and (c) *t* = 33nm.

C. Variation of junction resistance with barrier thickness

The junction resistance should be much reduced when pinholes are presented. In **Figure S7**, we plot the variation of resistance with different barrier thickness. The exponential increase of resistance with thickness clearly proves the tunneling behavior in our OMFTJ without pinhole contribution.

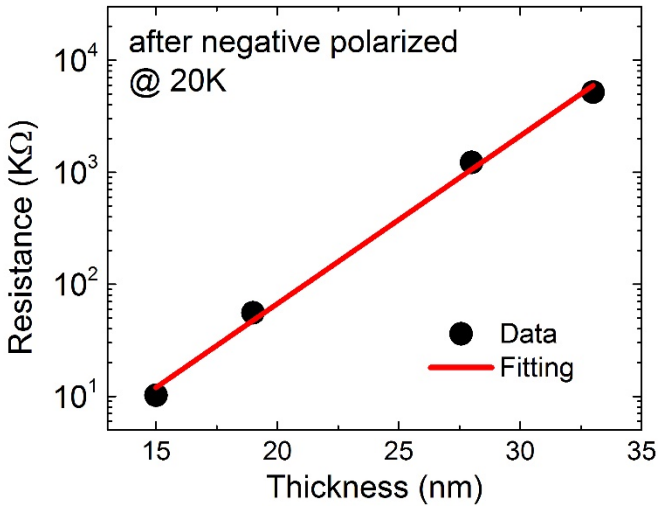

Figure S7. OMFTJ resistance (in negative polarization state, measured with a bias of +10mV) as a function of P(VDF-TrFE) thickness, which can be fitted with an exponential formula $R \propto \exp(at)$, where *t* is the barrier thickness, and *a* is the coefficient related to the barrier height.

S5. Anisotropic magnetoresistance in the ferromagnetic electrodes

To validate that the measured MR is not due to the AMR of FM electrodes, we have checked the AMR of LSMO and Co electrodes. As shown in **Figure S8,** the AMR of LSMO and Co shows a much smaller value lower than 0.4%. However, the MR in our device can be as large as 20%, which is much larger than that of AMR. We should also emphasize that the 20% MR well corresponds to the reported MR of 20% for $Co/Al_2O_3/STO/LSMO$ junctions.[1]

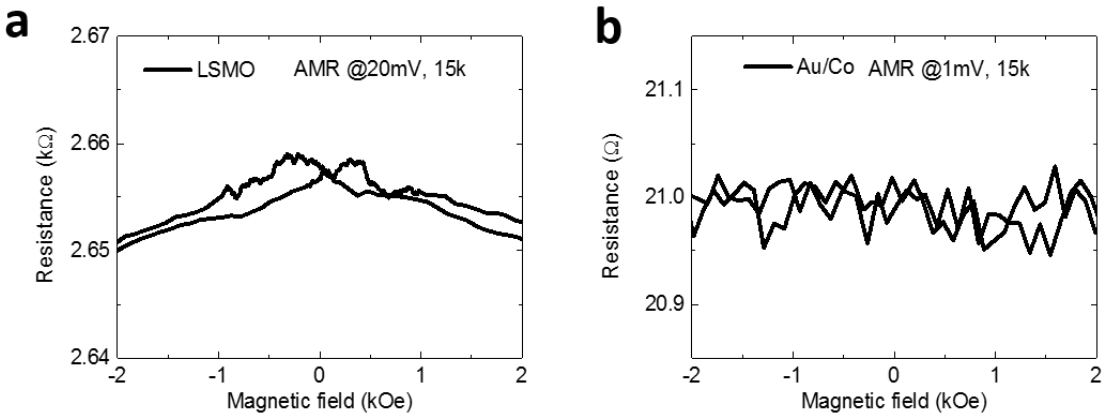

Figure S8. AMR measurement of (a) bottom LSMO and (b) top Au/Co electrodes.

Supporting Information References:

[1] Teresa, J.; Barthélémy, A.; Fert, A.; Contour, J. P.; Montaigne, F.; Seneor, P. Role of Metal-Oxide Interface in Determining the Spin Polarization of Magnetic Tunnel Junctions. *Science* **1999**, 286, 507.